Iranian Journal of Science and Technology, Transactions of Civil Engineering
https://doi.org/10.1007/s40996-023-01237-0

RESEARCH PAPER

Optimizing Grouting Techniques for Controlling Water Seepage, Using Rain Optimization Technique

Hojat Nouri[1] · **Ali Aalianvari**[1] · **Abbas Aghajani Bazzazi**[1]

Received: 14 June 2023 / Accepted: 8 September 2023

Abstract
The main objective of this paper is to use the rain optimization technique to improve the grouting process. Grouting is one of the most crucial techniques used to keep water out of tunnels. In this study, a new method was proposed to model the fracture and the surrounding rock when the fluid moves radially, providing a more accurate representation of the physical processes involved. In this paper the surrounding rock and a crack were initially simulated, and the constructed model was then solved using the rain optimization technique. To achieve this, the surrounding rock was separated into 30 blocks, and the fracture itself was divided into ten blocks. Nine different fluids were then injected into the crack, all of which had a time-dependent viscosity. In other words, their viscosity grew over time. One of these fluids was injected into the crack in the first stage at 5 different pressures and flow rates, and the minimum pressure that could be used to inject this fluid was determined to be 900 psi. Only fluids 4 and 5 were able to seal the fracture after the remaining 8 fluids were injected into the crack at a pressure of 900 psi. The majority of the fluids were unable to restrict the entry of water. Then, efforts were made to lower the injection pressure of fluids 4 and 5 as much as possible. The results showed that when fluid No. 4 is injected into the fracture at a pressure of 30 psi, it can seal the fracture, and when fluid No. 5 is injected into the gap at a pressure of 60 psi, it can regulate the inflow of water. To manage water inrush in tunnels, fluid No. 1 is recommended for high-pressure injection, while fluids Nos. 4 and 5 are recommended for low-pressure injection.

Keywords Matrix-fracture system · Fluid flow simulation · Water inrush control · Optimization

1 Introduction

Today, new issues and difficulties have arisen in the underground construction and mining sector due to the rising demand for constructing underground structures. One of these issues is the problem of water seepage into tunnels (Ge 2006). Studies have revealed that the inflow of water into tunnels can result in a wide range of significant issues. As this phenomenon is complicated and poorly understood, it can lead to terrible accidents and significant financial losses. Water ingress into tunnels can also diminish local subterranean water supplies, underground water levels, and eventually local water storage (Shucai 2016). Additionally, geological issues like tunnel wall collapse and ground surface fissures may occur in severe situations. Grouting operations are one of the newest techniques used to stop water from entering the mine. Significant efforts have been made in this area to enhance the setup requirements, methods of application, materials, and equipment. Although there are instances of injection procedures from the 1950s, actual study into this topic only began around 2000 (Katibeh and Aalianvari 2012). In order to carry out injection operations under dynamic subterranean water circumstances, Liu (2011) suggested a novel approach called VCH and assessed and analyzed its performance (Liu 2011). Due to the time dependence of the injection fluid's viscosity, they used cement–glass and cement–polymer injection fluids as two useful fluids in the injection operation for their experiments. They investigated the morphology of the contact surface of the injection fluid and water in a situation where underground water is considered to be dynamic. Despite much study in this area (Axelsson et al. 2009; Gothäll and Stille 2009; Mohammed et al. 2015; Rafi and Stille 2015; Sui 2015), accurate modeling and knowledge of slurry diffusion near running water in fractures and fissures have not

✉ Ali Aalianvari
ali_aalianvari@kashanu.ac.ir

[1] University of Kashan, Kashan, Islamic Republic of Iran

Published online: 16 October 2023

been provided. The determination of injection parameters, particularly injection pressure, and the design of injection operations are therefore entirely experimental. Water plugging operations in mines using the injection method are thus still entirely experimental and non-repetitive. Therefore, choosing the incorrect injection pressure can occasionally result in significant secondary issues, including rock instability, collapsing walls, and tunnel roofs (Nazari et al. 2023).

According to earlier studies (Xiao et al. 2010), acid sodium silicate-based grouts function rather well when there is low-flow surface water present. Conventional polyurethane grouts have reportedly undergone certain alterations, according to sources (Feng et al. 2013). The performance of this kind of grout has improved as a result of these improvements. However, the slurries needed for utilization under dynamic water conditions in a fracture have not received much attention in the literature. Since polymer slurries are expensive, acidic, and have limited action duration, they are rarely employed in dynamic water conditions nowadays. Therefore, it would appear that research into the various slurries that may be applied to these kinds of fractures is particularly crucial (Nazari et al. 2022).

Water ingress is a highly significant issue in underground mines because it can cause ground subsidence, pollution of subterranean water, changes in the effective stresses in the layers, and reductions in underground water levels. Previous studies have attempted to avoid these issues by presenting strategies for lowering water pressure by the digging of vertical holes and the submersible pumping of fluid outward. Although these techniques have occasionally been rather effective, a lot of focus has recently been placed on the technique of placing a cement curtain in the water channels to block them. Despite all the advancements achieved in this field, there are still many unanswered questions regarding this surgery. The design of cement slurry injection pressure and flow rate is entirely experimental and empirical, and occasionally it is accompanied by several mistakes. The best place for injection holes has not been identified, and it is uncertain how long-term use will affect how well injection grout membranes operate (Behnia et al. 2021).

In this study, we will attempt to optimize the pressure and flow rate of the injected fluid in the fracture by simulating the movement of injected fluid in a fracture with specified features near groundwater with low and high flow rates. The injectable volume of the slurry in a particular hole will also be established by taking into account the time-dependent features of the injecting grout, including the viscosity of the slurry. Based on this, the drilling position of the injection holes will be selected and optimized.

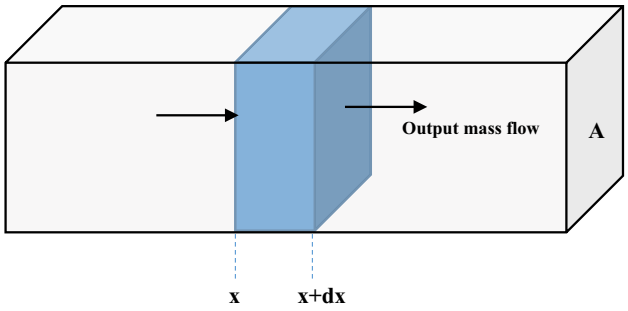

Fig. 1 The component taken into account for the mass balance of a single-phase fluid flow in a straightforward Cartesian one-dimensional model

2 Theory

The grouting procedure has seen considerable theoretical advancements and has garnered a lot of attention on a worldwide level. Studies on grouting theory have generally concentrated on the fluid and solid mechanics-based slurry movement in a crack, where slurry motion is examined in relation to variables including injection pressure, injection flow rate, diffusion, and injection time. The theories for injection include those for the amount of slurry penetration, the amount of adhesion produced by the injection, the amount of injection in joints, and the amount of injection in fractures. Despite the relatively extensive studies conducted in the field, the interaction between slurry and water, the impact of high flow rate water movement on injection operations, and the influence of time dependence on injection operations have not been thoroughly investigated, highlighting the need for further research in these areas (Shucai 2016; Gothäll and Stille 2010). The ideal flow rate and injection pressure to seal a fracture will be found as well as the best fluid that can be utilized in these settings after solving the equations that model the movement of the slurry in a crack.

2.1 Principles of simulating fluid movement in porous medium and cracks

A single-phase flow of an incompressible fluid with viscosity that varies with time is employed to inject the fluid into the crack, using three crucial equations—the continuity equation, the fluid flow equation in the porous media, and the equation of state—to simulate fluid motion in a porous medium and fracture.

Schiltz introduced the continuity equation in 1936, which provides a straightforward approach to simulating

fluid motion in a homogeneous container where the rock and fluid characteristics are identical. The continuity equation was derived using a simple one-dimensional model with single-phase fluid flow in a Cartesian coordinate system. Figure 1 depicts this problem in detail.

If there is no production or consumption in the element depicted in Fig. 1, the overall mass balance equation is as follows:

Input mass flow − Output mass flow = accumulation

$$\dot{m}_x.A.dt - \dot{m}_{x+dx}.A.dt = m_{t+dt} - m_t \tag{1}$$

The amount of mass in an element at time t is equal to the density of the fluid multiplied by the element volume. So:

$$\dot{m}_x.A.dt - \dot{m}_{x+dx}.A.dt = \left(\rho.A.dx.\emptyset\right)_{t+dt} - \left(\rho.A.dx.\emptyset\right)_t \tag{2}$$

In this equation:
$\dot{m}$: mass flow rate.
A: The cross section of the element.
dt: time changes.
m: mass.
ρ: fluid density.
dx: element length.
$\varnothing$: porosity.

Given the constant dt and dx, and the division of the sides of Eq. (2) by $dt.dx$, this relation is written as follows:

$$\frac{\dot{m}_x - \dot{m}_{x+dx}}{dx} = \frac{\left(\rho.\emptyset\right)_{t+dt} - \left(\rho.\emptyset\right)_t}{dt} \tag{3}$$

Considering:

$$\dot{m} = m/(A.dt) \tag{4}$$

$$m = \rho.v \tag{5}$$

And after replacing Eq. 5 in Eq. 4 we have:

$$\dot{m} = m.u \tag{6}$$

In these equations, v is the volume of the element, and u is the velocity of the fluid through the element. So by placing Eq. 6 in Eq. 3 and converting it to a differential form, we have:

$$-\frac{\delta\left(\rho u_x\right)}{\delta x} = \frac{\delta\left(\rho\emptyset\right)}{\delta t} \tag{7}$$

By following the same method, three-dimensional flow equation in the Cartesian system can be obtained as follows:

$$-\left(\frac{\delta\left(\rho u_x\right)}{\delta x} + \frac{\delta\left(\rho u_y\right)}{\delta y} + \frac{\delta\left(\rho u_z\right)}{\delta z}\right) = \frac{\delta\left(\rho\emptyset\right)}{\delta t} \tag{8}$$

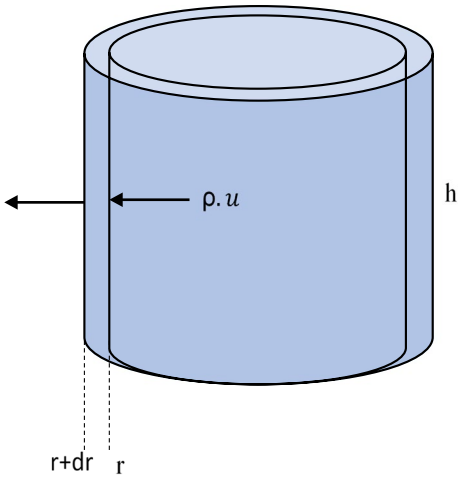

Fig. 2 Considered elements for mass flow balance of single-phase fluid in a one-dimensional model in a cylindrical system

Next, the mass balance equation for a one-dimensional single-phase flow in the direction of the radius in a cylindrical system (called a radial flow) will be expanded. In this case, the considered element to develop the mass balance equation is shown in Fig. 2.

Similarly, by writing the continuity equation for the shown element in Fig. 2, we have:

$$\dot{m}.A_r.dt - \dot{m}.A_{r+dr}.dt = \left(\rho.A.dr.\emptyset\right)_{t+dt} - \left(\rho.A.dr.\emptyset\right)_t \tag{9}$$

Given that in this system the cross section is $A = 2\pi rh$ and is a function of radius, so the mass balance equation is written as follows:

$$\frac{\dot{m}.r - \dot{m}.(r+dr)}{r.dr} = \frac{\left(\rho.\emptyset\right)_{t+dt} - \left(\rho.\emptyset\right)_t}{dt} \tag{10}$$

Therefore, the continuity equation in the radial system in differential form is written as follows:

$$-\frac{1}{r}\frac{\delta\left(r.\rho.u_r\right)}{\delta r} = \frac{\delta\left(\rho\emptyset\right)}{\delta t} \tag{11}$$

Single-phase laminar flow in macroscopic scales in a porous medium for one-dimensional flow in the horizontal system is defined by the Darcy equatiuon (1865) as follows:

$$u_x = \frac{q}{A} = -\frac{k_x}{\mu}\frac{dp}{dx} \tag{12}$$

In this equation, permeability (k) is in terms of square meters, viscosity (μ) is in Pa s, and velocity (u) is in terms of ms.

By placing the Darcy equation (Eq. 12) in Eq. 7, the following general equation for linear flow would be obtained:

$$\frac{\delta\left(\rho\frac{k_x}{\mu}\frac{\delta p}{\delta x}\right)}{\delta x}=\frac{\delta(\rho\emptyset)}{\delta t} \tag{13}$$

Since the fluid utilized in the grouting process is incompressible, the second side of Eq. 13 may be interpreted as zero because neither the fluid density nor the rock porosity will change over time. Consequently, the following equation will be utilized to model fluid motion in a porous material or fracture for linear flow:

$$\frac{\delta\left(\frac{k_x}{\mu}\frac{\delta p}{\delta x}\right)}{\delta x}=0 \tag{14}$$

Similarly, the final equation used to simulate the fluid flow in a porous medium or fracture for radial flow would be as follows:

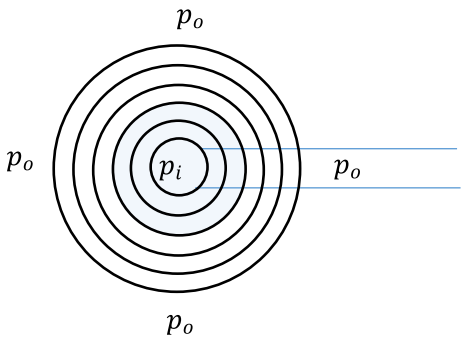

Fig. 3 The shape of a fracture when a borehole is drilled perpendicular to it and the radial motion of the injected fluid into the fracture

$$\frac{1}{r}\frac{\delta\left(r.\frac{k_r}{\mu}\frac{\delta p}{\delta r}\right)}{\delta r}=0 \tag{15}$$

2.2 Simulation of a fracture

To simulate the flow of an incompressible fluid in a fracture, two different modes can be considered:

1. The state that the walls on both sides of the fracture have zero permeability and the fluid cannot enter the matrix around the fracture.
2. The situation where the walls on both sides of the gap are a porous medium with a certain permeability and the injection fluid enters the matrix.

The first simulation is in fact a special case of the second case, and for a more comprehensive simulation, this case will be discussed in this study. Figure 3 shows a horizontal view of a fracture when fluid is injected into it from a hole:

Figure 3 shows that the fluid moves radially through the fracture. Each circle represents a block that must be precisely defined during the simulation. A vertical view of the shown section in Fig. 3, shows the blocks used in the simulation more precise (Fig. 4):

The simulation area is divided into a number of blocks, which are arranged in i rows and j columns, as seen in the vertical part of Fig. 4. The fluid may be transferred both horizontally and vertically between the blocks, each of which is in the shape of the shell of a cylinder. The radial model is used to describe the fluid's horizontal motion, and the linear model is used to describe the fluid's vertical motion. A pressure is assigned to the center of each block, which is denoted by $p\ (i, j)$ for the block in row i and column j.

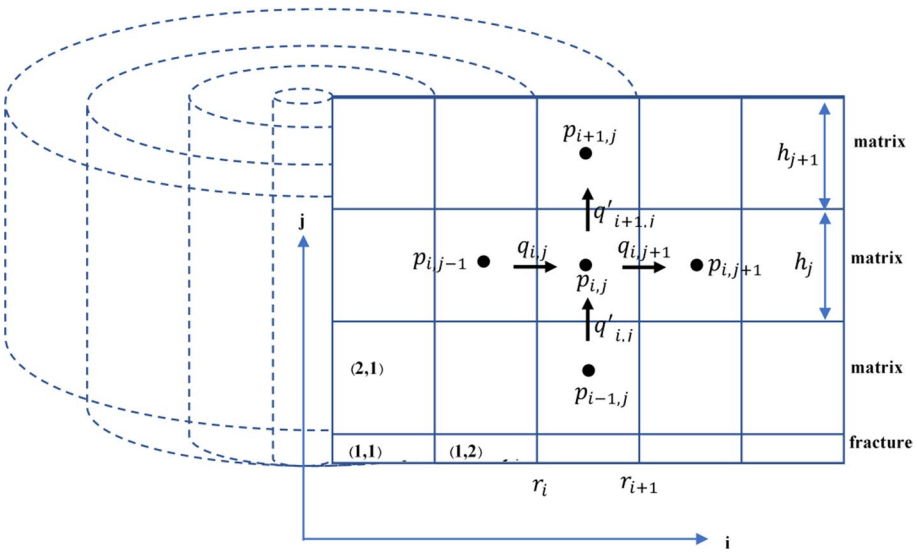

Fig. 4 Blocking used to simulate a fracture and the surrounding matrix in which each block will be seen as cylindrical shells

The fluid under pressure difference between the block and adjacent blocks may enter or leave a block from 4 directions. The fluid entering the block in the horizontal direction is shown with $q(i, j)$ and the output fluid from the block in the horizontal direction is shown $q(i, j+1)$. These two flows are calculated using the radial model. On the other hand, the input fluid to a block in the vertical direction is determined with $q(i, j)$, and the output fluid of a block in the vertical direction is denoted by $q(i+1, j)$. For ease of modeling, we assume that one side of the crack is impermeable and that the permeability of the opposite side is taken into account twice. Each block has specific properties that are predefined, such as its height, inner and outer radii, permeability in all directions, vertical and radial permeability, and viscosity of the fluid inside each block. The injection fluid's viscosity is a function of time and rises with time, which is a crucial aspect of this simulation.

2.3 Expansion of the linear flow equation

The linear flow equation was previously obtained as follows, and in this study, this equation will be used to calculate and simulate the vertical flow between blocks.

$$\frac{\delta\left(\frac{k_x}{\mu}\frac{\delta p}{\delta x}\right)}{\delta x} = 0$$

$$\frac{\delta\left(\frac{k_x}{\mu}\frac{\delta p}{\delta x}\right)}{\delta x} = \frac{\delta(q')}{\delta y} = q_{i,j}{}' - q_{i,j+1}{}' = 0$$

In this equation, q'_{ij} represents the vertical flow between two blocks, and its value is calculated from the following relation:

$$q'_{ij} = \frac{k'_{i,j}}{\mu(t)_{i,j}}\frac{p_{i,j-1} - p_{i,j}}{h} \tag{16}$$

$$q'_{ij+1} = \frac{k'_{i,j+1}}{\mu(t)_{i,j+1}}\frac{p_{i,j} - p_{i,j+1}}{h} \tag{17}$$

Also, to calculate and simulate the horizontal motion of the fluid between the blocks, we can use the extended equation for radial flow in the previous sections:

$$\frac{1}{r}\frac{\delta\left(r.\frac{k_r}{\mu}\frac{\delta p}{\delta r}\right)}{\delta r} = q$$

To simplify the equation, we assume that $\lambda(t) = \frac{k}{\mu(t)}$ and $R = r^2$. So the above equation will be simplified as follows:

$$4\frac{\delta\left(R.\lambda(t)\frac{\delta p}{\delta R}\right)}{\delta R} = q \tag{18}$$

If Eq. 18 is extended for block (i, j), we have:

$$\frac{4}{\Delta R}\left[\left(R_{i+\frac{1}{2}}\lambda_{i+\frac{1}{2},j}\frac{p_{i+1,j} - p_{i,j}}{R_{i+1,j} - R_{i,j}}\right) - \left(R_{i-\frac{1}{2}}\lambda_{i-\frac{1}{2},j}\frac{p_{i,j} - p_{i-1,j}}{R_{i,j} - R_{i-1,j}}\right)\right] = q \tag{19}$$

If we use logarithmic averaging to get the mean R in a block, we have:

$$R_{i+\frac{1}{2},j} = \frac{R_{i+1,j} - R_{i,j}}{ln\left(\frac{R_{i+1,j}}{R_{i,j}}\right)^2} = \frac{R_{i+1,j} - R_{i,j}}{2\ln\left(\frac{r_{i+1,j}}{r_{i,j}}\right)} \tag{20}$$

$$R_{i-\frac{1}{2},j} = \frac{R_{i,j} - R_{i-1,j}}{ln\left(\frac{R_{i,j}}{R_{i-1,j}}\right)^2} = \frac{R_{i,j} - R_{i-1,j}}{2\ln\left(\frac{r_{i,j}}{r_{i-1,j}}\right)} \tag{21}$$

Placing Eqs. (20) and (21) into Eq. (19) yields:

$$\frac{4}{\Delta R}\left[\left(\frac{R_{i+1,j} - R_{i,j}}{2\ln\left(\frac{r_{i+1,j}}{r_{i,j}}\right)}\lambda_{i+\frac{1}{2},j}\frac{p_{i+1,j} - p_{i,j}}{R_{i+1,j} - R_{i,j}}\right) - \left(\frac{R_{i,j} - R_{i-1,j}}{2\ln\left(\frac{r_{i,j}}{r_{i-1,j}}\right)}\lambda_{i-\frac{1}{2},j}\frac{p_{i,j} - p_{i-1,j}}{R_{i,j} - R_{i-1,j}}\right)\right] = q \tag{22}$$

Canceling common factors in both side of the above equation yields:

$$\frac{2}{\Delta R}\left[\left(\lambda_{i+\frac{1}{2},j}\frac{p_{i+1,j} - p_{i,j}}{\ln\left(\frac{r_{i+1,j}}{r_{i,j}}\right)}\right) - \left(\lambda_{i-\frac{1}{2},j}\frac{p_{i,j} - p_{i-1,j}}{\ln\left(\frac{r_{i,j}}{r_{i-1,j}}\right)}\right)\right] = q \tag{23}$$

Considering that there is no injection or production from any of the blocks, the value of q in each block is zero. So we have:

$$\left(\lambda_{i+\frac{1}{2},j}\frac{p_{i+1,j}-p_{i,j}}{\ln\left(\frac{r_{i+1,j}}{r_{i,j}}\right)}\right)-\left(\lambda_{i-\frac{1}{2},j}\frac{p_{i,j}-p_{i-1,j}}{\ln\left(\frac{r_{i,j}}{r_{i-1,j}}\right)}\right)=0 \tag{24}$$

Also, considering the value of radial permeability at the input boundary of the block (i, j) to be equal to $k_{i,j}$ and the value of radial permeability at the output boundary of this block to be equal to $k_{i+1,j}$ and similarly the value of the fluid viscosity at time t at the inlet and outlet boundaries of the block equal to $\mu(t)_{i,j}$ and $\mu(t)_{i+1,j}$, respectively, and multiplying two sides of relationship 24 by the height of the block yields:

$$\left(\frac{2\pi k_{i,j}h}{\mu(t)_{i,j}\ln\left(\frac{r_{i+1,j}}{r_{i,j}}\right)}p_{i+1,j}-p_{i,j}\right)-\left(\frac{2\pi k_{i+1,j}h}{\mu(t)_{i+1,j}\ln\left(\frac{r_{i,j}}{r_{i-1,j}}\right)}p_{i,j}-p_{i-1,j}\right)=0 \tag{25}$$

The first expression of the left side of relation 25 is exactly equal to the input flow to the block (i, j), and the second expression of the left side of relation 25 is exactly equal to the output flow of this block in radial flow. So:

$$q_{i,j}=\frac{2\pi k_{i,j}h}{\mu(t)_{i,j}\ln\left(\frac{r_{i+1,j}}{r_{i,j}}\right)}p_{i+1,j}-p_{i,j} \tag{26}$$

$$q_{i+1,j}=\frac{2\pi k_{i+1,j}h}{\mu(t)_{i+1,j}\ln\left(\frac{r_{i,j}}{r_{i-1,j}}\right)}p_{i,j}-p_{i-1,j} \tag{27}$$

$$q_{i,j}-q_{i+1,j}=0 \tag{28}$$

So for a specific block (i, j) we have:

$$q_{i,j}-q_{i+1,j}+q_{i,j}'-q_{i,j+1}'=0 \tag{29}$$

This condition must be checked for all blocks, and by simultaneously solving the system of equations obtained for all blocks, the pressure in each block can be calculated. For example, to solve the simulation of a fracture with $n\times n$ blocks, the following system of equations must be solved:

$$\begin{cases} q_{1,1}-q_{2,1}+q'_{1,1}-q'_{1,2}=0 \\ q_{1,2}-q_{2,2}+q'_{1,2}-q'_{1,3}=0 \\ \vdots \\ q_{i,j}-q_{i+1,j}+q'_{i,j}-q'_{i,j+1}=0 \\ \vdots \\ q_{n,n}-q_{n+1,n}+q'_{n,n}-q'_{n,n+1}=0 \end{cases}$$

2.4 Boundary conditions

Border conditions significantly affect how this challenge can be solved. In this investigation, it is assumed that a drill has pierced the matrix as necessary by passing vertically through a crack. The pump's injection pressure determines its value, and its upper limit, naturally, relies on the fracture pressure of the rock within the tunnel. As a result, the inlet fluid pressure to the fracture and the matrix is equal to $p_$in. The inlet flow from the matrix to the fracture from one side

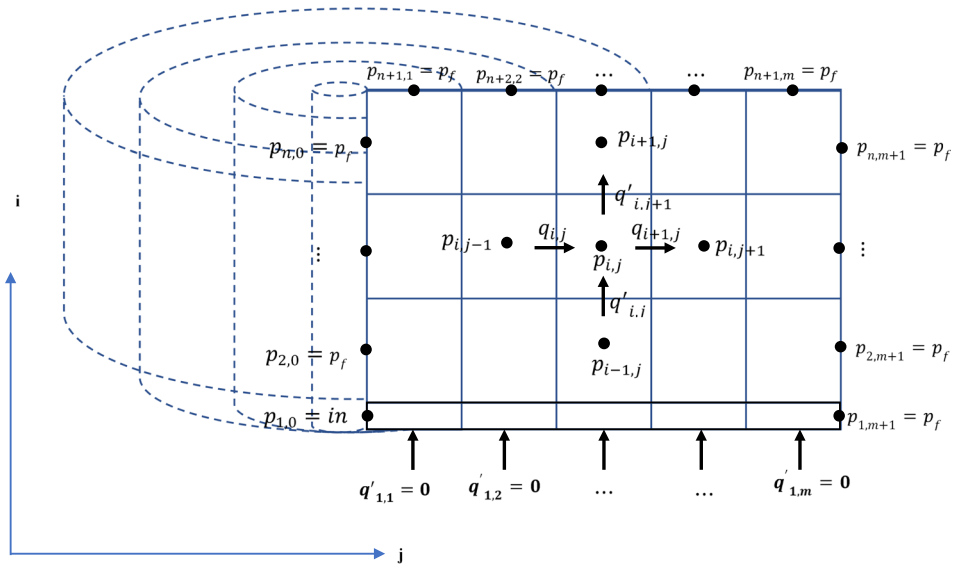

Fig. 5 The boundary conditions used for solving the model

is taken into consideration to be zero since we simulated the fracture from one side (in Fig. 5, the inlet flow from the bottom into the fracture is taken into consideration to be zero). The pressure on the other two sides of the model is equal to the water pressure in the formation. Figure 5 better illustrates the boundary conditions of the problem:

2.5 Calculate the pressure in each block

As previously mentioned, the pressure in each block can be determined by taking into account the boundary conditions and solving the system of equations outlined in the previous section. In this study, a novel meta-heuristic optimization technique called the rain optimization algorithm proposed to solve the system of equations. Using this approach, the pressure in each block estimated and the total flow determined by checking if it is zero in each block. This allows us to accurately determine the pressure in each block.

2.6 Calculate the input and output flow rates of each block

Having the pressure of adjacent blocks of each block, the inlet and outlet flow to each block can be easily calculated using the relations 16, 17, 26 and 27.

Determining the working front of the injected fluid.

Another problem is determining the locks that would be filled until the injection time $T = t$ and front of the injection fluid. To do this, the following steps can be done:

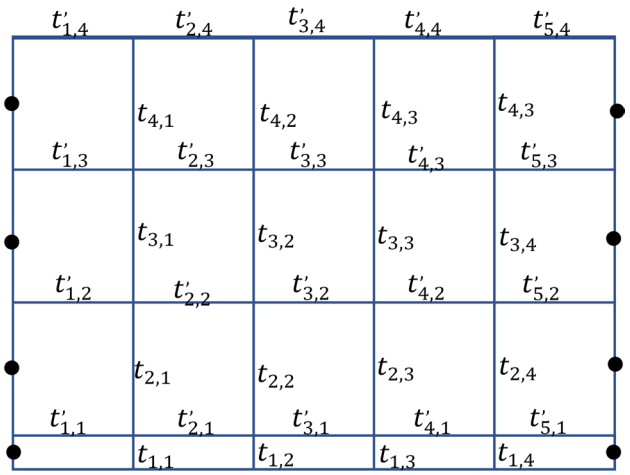

Fig. 6 Method for calculating the arrival time of the fluid front to the output boundaries of each block

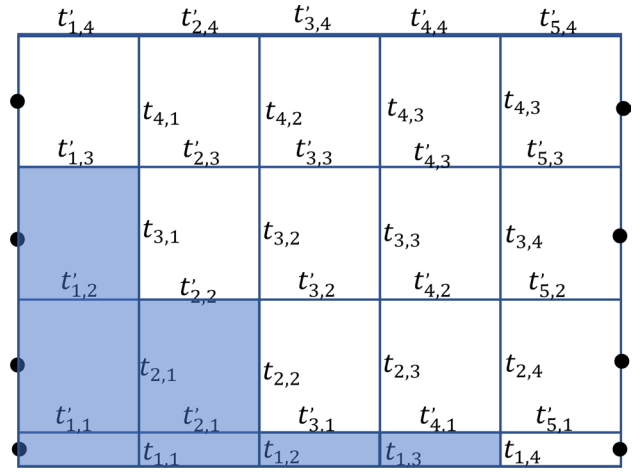

Fig. 7 The front of injected fluid in the model

1. Regardless of the time, a large model with a relatively large number of blocks should be considered and using the given method for the pressure calculation, the pressure and the inlet and outlet flow to each block can be calculated.
2. According to the injection flow rate to the first block and time t, the volume of fluid injected to the first block at time t is determined (v_1).
3. Is the volume of fluid injected at this time greater than the volume of the first block? If this is the case, then the fluid has left the first block from the other three directions. The flow rate of the fluid in the other three directions of the first block has already been calculated. Therefore, we calculate the filling time of the first block and subtract it from the total injection time $T\text{^},= T - t\_1$.
4. For adjacent blocks of the first block, repeat steps 2 and 3 and continue to do these steps until the sum of the total passage times of the fluid from each block in the direction of fluid movement exceeds the injection time.
5. In this way, on the boundary of each block, the time for the fluid to reach that boundary can be calculated. Figure 6 shows this Issue better.

In Fig. 6, assuming that the injection time t in the vertical direction is less than $t'_{1,3}$, and $t'_{2,2}$, and $t'_{3,1}$, and $t'_{4,1}$, and also in the horizontal direction the injection time t is less than $t_{3,1}$ and $t_{2,2}$ and $t_{1,4}$, then the front of the injected fluid will be as shown in Fig. 7:

2.7 Simulation of fluid motion considering the viscosity dependence of time

The pressure distribution in the blocks will have different values at various times due to the influence of viscosity on time. To get the precise front of the injected fluid, the

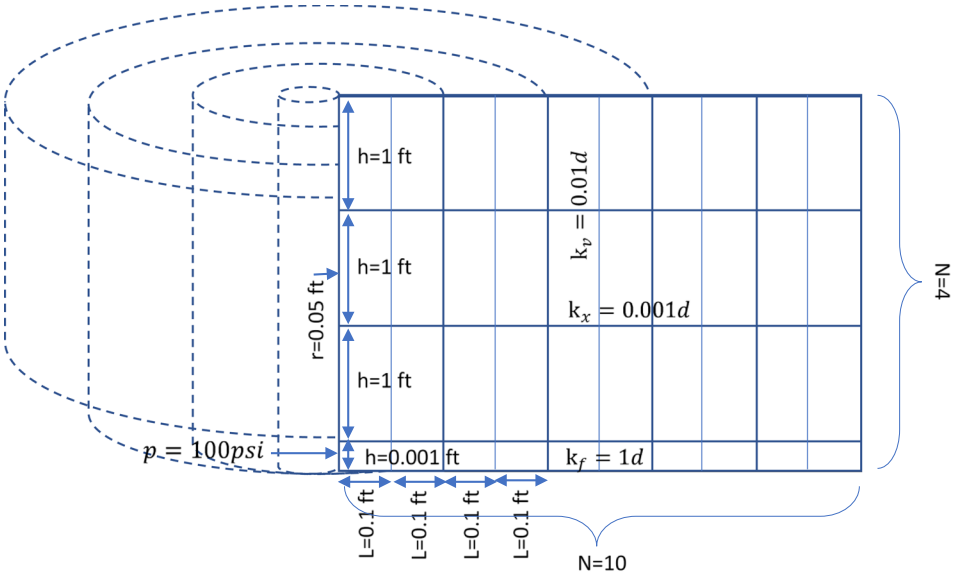

Fig. 8 Geometric and geophysical properties of the created model for simulation

Table 1 Calculated pressure in each block when a fluid with a viscosity of 1 centipoise and a pressure of 100psi is injected into the fracture

	Col. 1	Col. 2	Col. 3	Col. 4	Col. 5	Col. 6	Col. 7	Col. 8	Col. 9	Col. 10
Raw 3	10.17	10.10	10.08	10.06	10.05	10.03	10.03	10.02	10.02	10.02
Raw 2	10.34	10.19	10.15	10.12	10.09	10.07	10.05	10.04	10.03	10.03
Raw 1	10.32	10.27	10.23	10.18	10.14	10.11	10.08	10.06	10.05	10.05
Fracture	56.51	31.90	22.67	17.85	15.02	13.25	12.09	11.31	10.75	10.34

Table 2 Calculated horizontal flow between the blocks when a fluid with a viscosity of 1 centipoise and a pressure of 100psi is injected into the fracture

	Col. 1	Col. 2	Col. 3	Col. 4	Col. 5	Col. 6	Col. 7	Col. 8	Col. 9	Col. 10
Raw 3	8.43E−05	5.06E−05	5.60E−05	7.43E−05	8.08E−05	6.10E−05	5.27E−05	4.18E−05	1.08E−05	8.43E−05
Raw 2	1.78E−04	9.76E−05	1.11E−04	1.50E−04	1.64E−04	1.21E−04	1.06E−04	8.52E−05	1.96E−05	1.78E−04
Raw 1	6.01E−01	1.16E+00	1.64E+00	2.04E+00	2.29E+00	1.93E+00	2.01E+00	1.50E+00	3.12E−02	6.01E−01
Fracture	2.92E+00	2.35E+00	1.87E+00	1.47E+00	1.15E+00	9.00E−01	7.15E−01	5.85E−01	4.79E−01	2.92E+00

Table 3 Calculated vertical flow between the blocks when a fluid with a viscosity of 1 centipoise and a pressure of 100psi is injected into the fracture

	Col. 1	Col. 2	Col. 3	Col. 4	Col. 5	Col. 6	Col. 7	Col. 8	Col. 9	Col. 10
Raw 3	0.0022	0.0025	0.0029	0.0032	0.0030	0.0027	0.0024	0.0021	0.0019	0.0020
Raw 2	0.0022	0.0024	0.0029	0.0032	0.0030	0.0026	0.0024	0.0021	0.0019	0.0020
Raw 1	0.0018	0.0022	0.0030	0.0032	0.0034	0.0033	0.0030	0.0023	0.0018	0.0023
Fracture	0.6016	0.5634	0.4861	0.3992	0.3173	0.2453	0.1832	0.1298	0.0819	0.0378

process of trial and error must be applied. The fluid front of the blocks would be established in each of the many time steps that would be employed for this purpose. The injected fluid can nevertheless go farther with passing time if the pressure inside the boundary blocks is higher than the pressure of the fluid outside the block. As a result, we extend the injection period by an additional time step and, at this point, we once again calculate the pressure of each block and the fluid's front. Until the pressure inside the boundary blocks is greater than the pressure outside, this procedure

would be carried out continually. The injectable fluid now solidifies in this location since it can no longer travel.

3 Discussion

A 10-by-4 grid was employed for the simulation, with each cylinder being partitioned into 4 blocks and 10 nested cylindrical blocks. The vertical blocks' height was equivalent to one foot, while the fracture opening's diameter was 0.001 feet. Each cylindrical block was also thought to have a thickness of 0.1 feet. According to this model, the horizontal and vertical permeability of each matrix block were set at 0.001 and 0.01 Darcy, respectively, and the fracture permeability was set at 10 Darcy. On the other hand, the initial pressure of the water in the blocks before injection was thought to be equivalent to 10 psi, whereas the pressure of the fluid that was injected into the crack was equal to 100 psi. This block size is better seen in Fig. 8. This model was made simpler by duplicating the vertical permeability of the blocks and setting the permeability of one side of the fracture (the bottom of the fracture) to zero.

The pressure in the middle of each block was determined after the model developed for this study was solved using the rain optimization technique. For this, the fluid viscosity of 1cp was taken into account. Table 1 shows the pressure attained in each block using the rain optimization method after 100 iterations of choosing a starting population of 50. Table 2 provides the horizon flow between the blocks, whereas Table 3 provides the vertical flow between the blocks.

Table 4 Filling time of each block (from the start of injection process in seconds) when a fluid with a viscosity of 1 cp and a pressure of 100 psi is injected into the fracture

	Col. 1	Col. 2	Col. 3	Col. 4	Col. 5	Col. 6	Col. 7	Col. 8	Col. 9	Col. 10
Raw 3	772,437.3	310,449.5	362,265.7	444,867.7	559,196.6	733,799.8	946,128.7	1,296,933.9	1,718,514.1	1,606,682.3
Raw 2	851,528.3	164,979.6	181,294.7	221,824.4	266,334.2	330,076.8	424,241.1	626,155.2	874,892.2	722,162.7
Raw 1	296.1	633.0	1092.1	1524.5	1961.4	2427.9	3073.2	3780.9	4846.2	52,142.3
Fracture	0.5	1.7	4.0	7.8	13.9	23.2	37.0	56.9	84.2	121.4

Table 5 Fluids with time-dependent viscosity used in this simulation

Types of slurry	Water–cement ratio of cement grouting	Volume ratio	Equations of time-dependent viscosity	Scope application
Cement–sodium silicate slurry	1:1	1:1	$\mu_1 = 0.003182t^{2.23}$	t = 0–180 s; T = 20 °C; no additives
		2:1	$\mu_2 = 0.008427t^{2.694}$	
		3:1	$\mu_3 = 0.01864t^{2.066}$	
	2:1	1:1	$\mu_4 = 1.422 \times 10^{-8}t^{4.215}$	
		2:1	$\mu_5 = 4.763 \times 10^{-6}t^{3.173}$	
Polymer modification materials	1:1	1:1	$\mu_6 = -7.89 \times 10^{-8}t^3 - 0.003195t^2 + 0.4467t + 0.6$	
		2:1	$\mu_7 = -1.005 \times 10^{-7}t^4 - 4.198 \times 10^{-5} - 0.008976t^2 + 0.6848t + 0.3$	
	2:1	1:1	$\mu_8 = 1.362 \times 10^{-6}t^3 - 8.608 \times 10^{-4} - 0.008976t^2 - 0.2046t + 0.5$	
		2:1	$\mu_9 = 4.303 \times 10^{-6}t^3 - 0.001705t^2 + 0.2378t + 0.5$	

Table 6 Filling time of each block (from the start of injection process in seconds) when a fluid no. 1 is injected into the fracture with a pressure of 100 psi

	Col. 1	Col. 2	Col. 3	Col. 4	Col. 5	Col. 6	Col. 7	Col. 8	Col. 9	Col. 10
Raw 3	Inf	Inf	Inf	Inf	Inf	Inf	Inf	Inf	Inf	Inf
Raw 2	Inf	Inf	Inf	Inf	Inf	Inf	Inf	Inf	Inf	Inf
Raw 1	86.6	902.6	Inf	Inf	Inf	Inf	Inf	Inf	Inf	Inf
Fracture	0.3	0.7	3.9	261.2	Inf	Inf	Inf	Inf	Inf	Inf

Table 7 Calculated pressure in each block when fluid no. 1 is injected to the block with a pressure of 300psi

	Col. 1	Col. 2	Col. 3	Col. 4	Col. 5	Col. 6	Col. 7	Col. 8	Col. 9	Col. 10
Raw 3	10.33	10.51	10.22	10.14	10.10	10.06	10.03	10.01	10.00	10.00
Raw 2	10.64	11.05	10.42	10.29	10.20	10.13	10.07	10.02	10.01	10.01
Raw 1	10.89	10.72	10.58	10.44	10.31	10.20	10.11	10.03	10.01	10.01
Fracture	159.58	80.09	50.24	34.61	25.42	19.63	15.89	13.54	12.00	10.89

Table 8 Filling time of each block (from the start of injection process in seconds) when a fluid no. 1 is injected into the fracture with a pressure of 300 psi

	Col. 1	Col. 2	Col. 3	Col. 4	Col. 5	Col. 6	Col. 7	Col. 8	Col. 9	Col. 10
Raw 3	Inf	Inf	Inf	Inf	Inf	Inf	Inf	Inf	Inf	Inf
Raw 2	Inf	Inf	Inf	Inf	Inf	Inf	Inf	Inf	Inf	Inf
Raw 1	62.16	331.62	4743.07	Inf	Inf	Inf	Inf	Inf	Inf	Inf
Fracture	0.50	0.75	1.93	18.12	3812.86	Inf	Inf	Inf	Inf	Inf

Table 9 Calculated pressure in each block when fluid no. 1 is injected to the block with a pressure of 600psi

	Col. 1	Col. 2	Col. 3	Col. 4	Col. 5	Col. 6	Col. 7	Col. 8	Col. 9	Col. 10
Raw 3	10.54	10.44	10.34	10.25	10.16	10.09	10.02	10.00	10.00	10.01
Raw 2	11.09	10.88	10.69	10.51	10.33	10.18	10.04	10.01	10.01	10.02
Raw 1	11.67	11.34	11.04	10.78	10.54	10.34	10.19	10.05	10.03	10.03
Fracture	315.31	153.86	93.56	61.68	43.01	31.16	23.47	18.31	14.67	12.10

Table 10 Filling time of each block (from the start of injection process in seconds) when a fluid no. 1 is injected into the fracture with a pressure of 600 psi

	Col. 1	Col. 2	Col. 3	Col. 4	Col. 5	Col. 6	Col. 7	Col. 8	Col. 9	Col. 10
Raw 3	Inf	Inf	Inf	Inf	Inf	Inf	Inf	Inf	Inf	Inf
Raw 2	Inf	Inf	Inf	Inf	Inf	Inf	Inf	Inf	Inf	Inf
Raw 1	6.49	16.89	45.22	172.68	1581.56	Inf	Inf	Inf	Inf	Inf
Fracture	0.25	0.27	0.33	0.49	1.08	6.29	404.93	Inf	Inf	Inf

Table 11 Calculated pressure in each block when fluid no. 1 is injected to the block with a pressure of 900 psi

	Col. 1	Col. 2	Col. 3	Col. 4	Col. 5	Col. 6	Col. 7	Col. 8	Col. 9	Col. 10
Raw 3	10.49	10.34	10.19	10.06	9.97	10.00	10.01	10.00	10.00	10.00
Raw 2	10.99	10.68	10.39	10.13	9.94	10.00	10.02	10.01	10.01	10.01
Raw 1	11.55	11.06	10.64	10.26	10.17	10.07	10.04	10.03	10.01	10.01
Fracture	468.03	223.29	131.22	82.76	53.87	36.09	24.46	15.97	11.15	10.52

Table 12 Filling time of each block (from the start of injection process in seconds) when a fluid no. 1 is injected into the fracture with a pressure of 900 psi

	Col. 1	Col. 2	Col. 3	Col. 4	Col. 5	Col. 6	Col. 7	Col. 8	Col. 9	Col. 10
Raw 3	Inf	Inf	Inf	Inf	Inf	Inf	Inf	Inf	Inf	Inf
Raw 2	Inf	Inf	Inf	Inf	Inf	Inf	Inf	Inf	Inf	Inf
Raw 1	1.80	4.03	8.26	18.51	52.53	243.66	3413.87	Inf	Inf	Inf
fracture	0.16	0.17	0.18	0.21	0.27	0.42	1.06	7.69	968.31	Inf

3.1 Determining the front of the injection fluid

To obtain the working front of the injected fluid at any given time t, it is sufficient to determine the blocks that are filled by the fluid at that time. If the fluid has a constant viscosity (in this modeling equal to 1cp) the filling time of each block will be according to Table 4:

Table 13 Calculated pressure in each block when fluid no. 1 is injected to the block with a pressure of 1200psi

	Col. 1	Col. 2	Col. 3	Col. 4	Col. 5	Col. 6	Col. 7	Col. 8	Col. 9	Col. 10
Raw 3	10.92	10.72	10.52	10.35	10.16	10.06	10.04	10.01	10.01	10.01
Raw 2	11.87	11.44	11.05	10.70	10.31	10.11	10.08	10.01	10.01	10.02
Raw 1	12.86	12.19	11.60	11.09	10.60	10.25	10.14	10.04	10.04	10.04
Fracture	623.95	297.86	175.47	111.49	73.88	50.20	34.59	23.67	15.50	12.48

Table 14 Filling time of each block (from the start of injection process in seconds) when a fluid no. 1 is injected into the fracture with a pressure of 1200 psi

	Col. 1	Col. 2	Col. 3	Col. 4	Col. 5	Col. 6	Col. 7	Col. 8	Col. 9	Col. 10
Raw 3	Inf	Inf	Inf	Inf	Inf	Inf	Inf	Inf	Inf	Inf
Raw 2	24,106.84	Inf	Inf	Inf	Inf	Inf	Inf	Inf	Inf	Inf
Raw 1	0.77	1.57	2.89	5.42	11.12	27.51	98.83	760.86	Inf	Inf
Fracture	Inf	Inf	Inf	Inf	Inf	Inf	Inf	Inf	Inf	Inf

Table 15 Filling time of each block (from the start of injection process in seconds) when a fluid no. 1 is injected into the fracture with a pressure of 900 psi

	Col. 1	Col. 2	Col. 3	Col. 4	Col. 5	Col. 6	Col. 7	Col. 8	Col. 9	Col. 10
Raw 3	Inf	Inf	Inf	Inf	Inf	Inf	Inf	Inf	Inf	Inf
Raw 2	Inf	Inf	Inf	Inf	Inf	Inf	Inf	Inf	Inf	Inf
Raw 1	1.80	4.03	8.26	18.51	52.53	243.66	3413.87	Inf	Inf	Inf
Fracture	0.16	0.17	0.18	0.21	0.27	0.42	1.06	7.69	968.31	Inf

Table 16 Filling time of each block (from the start of injection process in seconds) when a fluid no. 2 is injected into the fracture with a pressure of 900 psi

	Col. 1	Col. 2	Col. 3	Col. 4	Col. 5	Col. 6	Col. 7	Col. 8	Col. 9	Col. 10
Raw 3	Inf	Inf	Inf	Inf	Inf	Inf	Inf	Inf	Inf	Inf
Raw 2	Inf	Inf	Inf	Inf	Inf	Inf	Inf	Inf	Inf	Inf
Raw 1	26.21	100.89	696.83	37,533.85	Inf	Inf	Inf	Inf	Inf	Inf
Fracture	0.43	0.53	0.89	3.25	126.97	Inf	Inf	Inf	Inf	Inf

Table 17 Filling time of each block (from the start of injection process in seconds) when a fluid no. 3 is injected into the fracture with a pressure of 900 psi

	Col. 1	Col. 2	Col. 3	Col. 4	Col. 5	Col. 6	Col. 7	Col. 8	Col. 9	Col. 10
Raw 3	Inf	Inf	Inf	Inf	Inf	Inf	Inf	Inf	Inf	Inf
Raw 2	Inf	Inf	Inf	Inf	Inf	Inf	Inf	Inf	Inf	Inf
Raw 1	501.42	11,613.13	Inf	Inf	Inf	Inf	Inf	Inf	Inf	Inf
Fracture	0.95	3.00	44.10	17,879.50	Inf	Inf	Inf	Inf	Inf	Inf

Table 18 Filling time of each block (from the start of injection process in seconds) when a fluid no. 4 is injected into the fracture with a pressure of 900 psi

	Col. 1	Col. 2	Col. 3	Col. 4	Col. 5	Col. 6	Col. 7	Col. 8	Col. 9	Col. 10
Raw 3	1.83	2.18	2.88	4.56	8.58	29.89	103.85	3737.87	68,720.18	Inf
Raw 2	1.25	1.30	1.38	1.51	1.67	2.11	2.39	4.87	7.07	Inf
Raw 1	1.00	1.00	1.00	1.00	1.00	1.00	1.00	1.01	1.01	1.07
Fracture	1.00	1.00	1.00	1.00	1.00	1.00	1.00	1.00	1.00	1.00

If the viscosity of the fluid is a function of time, the filling time of the blocks by the injected fluid will be different. If fluid # 1 is selected as the injection fluid in Table 4, the filling time of the blocks will be much longer. Table 6 shows the filling time of each block when fluid number 1 in Table 5 is used:

Table 19 Filling time of each block (from the start of injection process in seconds) when a fluid no. 5 is injected into the fracture with a pressure of 900 psi

	Col. 1	Col. 2	Col. 3	Col. 4	Col. 5	Col. 6	Col. 7	Col. 8	Col. 9	Col. 10
Raw 3	Inf	Inf	Inf	Inf	Inf	Inf	Inf	Inf	Inf	Inf
Raw 2	128.43	234.39	507.04	1308.92	3830.76	17,370.51	Inf	Inf	Inf	Inf
Raw 1	1.14	1.31	1.54	1.90	2.46	3.37	4.91	7.69	13.64	31.42
Fracture	1.00	1.00	1.00	1.00	1.01	1.01	1.02	1.03	1.05	1.07

Table 20 Filling time of each block (from the start of injection process in seconds) when a fluid no. 6 is injected into the fracture with a pressure of 900 psi

	Col. 1	Col. 2	Col. 3	Col. 4	Col. 5	Col. 6	Col. 7	Col. 8	Col. 9	Col. 10
Raw 3	Inf	Inf	Inf	Inf	Inf	Inf	Inf	Inf	Inf	Inf
Raw 2	Inf	Inf	Inf	Inf	Inf	Inf	Inf	Inf	Inf	Inf
Raw 1	Inf	Inf	Inf	Inf	Inf	Inf	Inf	Inf	Inf	Inf
Fracture	54.09	1792.55	Inf	Inf	Inf	Inf	Inf	Inf	Inf	Inf

Table 21 Filling time of each block (from the start of injection process in seconds) when a fluid no. 7 is injected into the fracture with a pressure of 900 psi

	Col. 1	Col. 2	Col. 3	Col. 4	Col. 5	Col. 6	Col. 7	Col. 8	Col. 9	Col. 10
Raw 3	Inf	Inf	Inf	Inf	Inf	Inf	Inf	Inf	Inf	Inf
Raw 2	Inf	Inf	Inf	Inf	Inf	Inf	Inf	Inf	Inf	Inf
Raw 1	Inf	Inf	Inf	Inf	Inf	Inf	Inf	Inf	Inf	Inf
Fracture	50.66	2281.22	Inf	Inf	Inf	Inf	Inf	Inf	Inf	Inf

Table 22 Filling time of each block (from the start of injection process in seconds) when a fluid no. 8 is injected into the fracture with a pressure of 900 psi

	Col. 1	Col. 2	Col. 3	Col. 4	Col. 5	Col. 6	Col. 7	Col. 8	Col. 9	Col. 10
Raw 3	Inf	Inf	Inf	Inf	Inf	Inf	Inf	Inf	Inf	Inf
Raw 2	Inf	Inf	Inf	Inf	Inf	Inf	Inf	Inf	Inf	Inf
Raw 1	Inf	Inf	Inf	Inf	Inf	Inf	Inf	Inf	Inf	Inf
Fracture	15.99	382.31	Inf	Inf	Inf	Inf	Inf	Inf	Inf	Inf

Table 23 Filling time of each block (from the start of injection process in seconds) when a fluid no. 9 is injected into the fracture with a pressure of 900 psi

	Col. 1	Col. 2	Col. 3	Col. 4	Col. 5	Col. 6	Col. 7	Col. 8	Col. 9	Col. 10
Raw 3	Inf	Inf	Inf	Inf	Inf	Inf	Inf	Inf	Inf	Inf
Raw 2	Inf	Inf	Inf	Inf	Inf	Inf	Inf	Inf	Inf	Inf
Raw 1	Inf	Inf	Inf	Inf	Inf	Inf	Inf	Inf	Inf	Inf
Fracture	38.45	942.59	Inf	Inf	Inf	Inf	Inf	Inf	Inf	Inf

Table 6 shows numbers greater than 86,400 s (24 h) as Inf or infinite time, indicating that these blocks will not be saturated by the injection fluid even after 24 h of injection.

3.2 Injection pressure optimization

In this work, the simulation is used to determine the best fluid type and injection circumstances for sealing the crack. This implies that the injection pressure, flow rate, and fluid type should all be chosen to ensure that the fluid completely seals the crack. To put it another way, the fluid should be able to flow to the fracture's terminus and solidify as quickly as feasible. Table 6 demonstrates that under the prior injection settings, only the first four blocks of the crack were filled with fluid, leaving the remaining space free. In order to enhance these circumstances, the injection pressure was raised in 4 stages to the fracture's maximum tolerated pressure (1200 psi is taken into account in this study), and the model was used to determine the pressure of the blocks and the time it took to fill the blocks.

Step 1: Injection pressure equal to 300psi (Tables 7, 8).

Step 2: Injection pressure equal to 600psi (Tables 9, 10).

Table 24 Filling time of each block (from the start of injection process in seconds) when a fluid no. 5 is injected into the fracture with a pressure of 60 psi

	Col. 1	Col. 2	Col. 3	Col. 4	Col. 5	Col. 6	Col. 7	Col. 8	Col. 9	Col. 10
Raw 3	Inf	Inf	Inf	Inf	Inf	Inf	Inf	Inf	Inf	Inf
Raw 2	Inf	Inf	Inf	Inf	Inf	Inf	Inf	Inf	Inf	Inf
Raw 1	3.58	6.74	11.72	20.68	38.89	83.50	235.47	1241.49	38,936.61	Inf
Fracture	1.00	1.01	1.04	1.07	1.14	1.26	1.51	2.18	5.42	83.16

Table 25 Filling time of each block (from the start of injection process in seconds) when a fluid no. 4 is injected into the fracture with a pressure of 30 psi

	Col. 1	Col. 2	Col. 3	Col. 4	Col. 5	Col. 6	Col. 7	Col. 8	Col. 9	Col. 10
Raw 3	Inf	Inf	Inf	Inf	Inf	Inf	Inf	Inf	Inf	Inf
Raw 2	Inf	Inf	Inf	Inf	Inf	Inf	Inf	Inf	Inf	Inf
Raw 1	5.53	9.90	16.84	29.33	54.74	117.48	335.01	1943.76	Inf	Inf
Fracture	1.00	1.01	1.04	1.09	1.02	1.45	2.68	3.63	8.35	231.47

Step 3: Injection pressure equal to 900psi (Tables 11, 12).

Step 4: Injection pressure equal to 1200psi (Tables 13, 14).

Although by injection with a pressure of 1200 psi all the blocks of the fracture are sealed by the injection fluid, this amount of pressure is equal to the maximum pressure that can be used in the injection operation. Therefore, it is suggested to consider a safety factor of 0.25 and try to seal all the blocks by injecting fluid at 900 psi.

3.3 Optimal fluid selection

B. In this study, we attempted to employ nine different fluids for injection operations whose viscosity depended on time. Table 5 displays the relationships between these fluids and time that depend on them. According to the kind of fluid employed, Tables 15, 16, 17, 18, 19, 20, 21, 22 and 23 display the filling times for the blocks used in the simulation. The pressure utilized for injection is 900 psi, and it should be noted that all of the simulation parameters are comparable to those listed in section.

According to Table 15, fluid 1 can quickly seal the first 8 columns of the gap at 900 psi in about 8 s, but it takes about 968 s to close the ninth column, and at this pressure, the fluid would not be able to seal the last block. Although Table 14 shows that this fluid may seal all ten columns associated with the crack in 73 s when injected at a pressure of 1200 psi, taking into account that at this pressure, blocks may form, The usage of this pressure when moving on the mine's walls and ceiling is not advised. Fluids No. 2 and 3, when injected at a pressure of 900 psi, are only able to seal the first 4 blocks of the fracture, and the fracture would be sealed before getting the injection fluid to the end of the fracture. Although these fluids will be able to penetrate more into the fracture by increasing the injection pressure, but it is clear that in the used pressure range in this simulation, it is not possible to use them.

Fluids 4 and 5, are able to reach the end of the gap very quickly (less than 2 s) when injected at 900 psi. This shows that they can be injected into the gaps with a lower flow rate and pressure. In the next section, the feasibility of using these two fluids at lower pressures will be investigated.

Fluids 6 to 9, fill only the first two blocks of the fracture when injected at 900 psi, indicating that these four fluids are not suitable for this simulation.

3.4 Selecting the best injection pressure for fluids no. 4 and 5

Table 24 shows that fluids 4 and 5 may also be employed in this simulation with lesser injection pressure. To do this, the minimal injection pressure needed to close the crack was calculated by gradually lowering the injection pressure for these two fluids. At a pressure of 60 psi, Fluid No. 5 may be readily injected into the crack, and it will take no longer than 83 s to completely seal it. The following table displays the injection time of fluid No. 5 at a 60 psi injection pressure:

In the case of fluid No. 4, as shown in Table 25, the minimum injection pressure to seal the fracture is 30 psi.

4 Results

The simulation yielded several significant outcomes, including:

1. A new method was proposed to model the fracture and the surrounding rock when the fluid moves radially, pro-

viding a more accurate representation of the physical processes involved.

2. The rain optimization algorithm was used to solve the created model with high accuracy, demonstrating the effectiveness of meta-heuristic methods for solving numerical models.
3. The viscosity of the injected fluid was considered as a function of time, and nine different fluids with varying viscosity models were used to simulate the fluid injection process. A method was also developed to locate the front of the injection fluid.
4. Only three of the nine fluids used in the simulation (fluids 1, 4, and 5) were able to effectively seal the modeled fracture, while the remaining fluids were stopped before reaching the end of the fracture.
5. Fluid number 1, when injected into the fracture at a pressure of 900psi, was able to almost completely seal the fracture and halt the movement of water. In contrast, fluids 4 and 5 were able to achieve similar results at much lower pressures (60psi and 30psi, respectively).

References

Axelsson M, Gustafson G, Fransson Å (2009) Stop mechanism for cementitious grouts at. Tunn Undergr Space Technol 24(4):390–397

Behnia B, AaliAnvari A, Nazari MH (2021) A study to examine the effect of grouting superfine cement slurry containing nano-silica additives by a simulator cylinder in environments with many joints and gaps. Arab J Geosci 14:1–15

Feng Z, Kang HP, Han GQ (2013) Polyurethane grouting materials modified by inorganic salts in coal mines. Chin J Geotechn Eng 35(8):1559–1564 ((**in Chinese**))

Ge J (2006) Development and prospects of chemical grouting techniques. Chin J Rock Mech Eng 25(2):3384–3392

Gothäll R, Stille H (2009). Fracture dilation during grouting. Tunn Undergr Space Technol 24(2):126e35.

Gothäll R, Stille H (2010) Fractureefracture interaction during grouting. Tunn Undergr Space Technol 25(3):199–204

Katibeh H, Aalianvari A (2012) Common Approximations to the water inflow into Tunnels. Drainage Syst 75–88

Liu R (2011) Mechanism study and application of cement-based fast curing grouts in underground construction dynamic grouting defusion and plugging method. Shanghai University.

Mohammed HM, Pusch R, Knutsson S (2015) Study of cement-grout penetration into fractures. Tunnell Undergr Space Technol 45:10–19

Nazari MH, Uromeie A, Aalianvari A (2022) Study of rapid filtration of cement based grouts by a steel model in the field. Geotech Geol Eng 40(7):3827–3838

Nazari MH, Uromeie A, Aalianvari A (2023) Coupled grout flow: fracture deformation effects on grout penetration in a physical model. Iran J Sci 47(3):765–777

Rafi J, Stille H (2015) Basic mechanism of elastic jacking and impact of fracture aperture. Tunnell Undergr Space Technol 49:174e87.

Shucai LL (2016) Protection against water or mud inrush in tunnels by grouting: a rewiev. J Rock Mech Geotechn Eng 8:753–766

Sui W et al. (2015) Experimental investigation on sealing efficiency of chemical grouting in rock fracture with flowing water. Tunn Undergr Space Technol 50:239–249

Xiao Z et al. (2010) Calcium carbonic acid-acid water glass grouting material and comparing test. J Central South Univ 41(6):2305–2312